Communications

Layered Silicates by Swelling of AMH-3 and Nanocomposite Membranes**

Sunho Choi, Joaquin Coronas, Edgar Jordan, Weontae Oh, Sankar Nair, Frank Onorato, Daniel F. Shantz, and Michael Tsapatsis*

Layered materials with nanoporous layers (e.g., MCM-22(P),[1–4] AMH-3[5,6]) have structures intermediate between those of crystalline nanoporous frameworks, such as zeolites, and typical layered materials, such as clay minerals. Each layer includes a porous network, while the gallery between layers provides the ability for intercalation, pillaring, and exfoliation.[3–5,7–13] One such material, AMH-3, is the first layered silicate with internal porosity accessible from all directions through eight-membered ring (8 MR) apertures (i.e. pore openings made of eight SiO_4 tetrahedra).[5,6] It has been proposed to use exfoliated silicate layers of AMH-3 as a selectivity-enhancing additive in polymers.[14,15] A recent simulation study provides further motivation for the fabrication of nanocomposites incorporating dispersed AMH-3

layers for gas separation membranes.[16] However, fabrication of nanocomposites has not been demonstrated. Herein, we report on AMH-3 swelling using a novel procedure; the swollen material is used to prepare polymer nanocomposite membranes with improved selectivity.

Typically, layered materials can be swollen by the intercalation of organic surfactants, such as quaternary alkyl ammonium ions or amine molecules, by cation exchange or hydrogen-bonding interaction with intergallery moieties.[3,4,17–24] The swollen derivative of AMH-3 was prepared by intercalation of primary amine molecules (dodecylamine) after proton exchange in the presence of amino acid. In this procedure, an aqueous solution of DL-histidine was employed as a buffer and a source of protons to exchange the strontium and sodium cations in the original structure. The initial pH value was adjusted to be approximately 6.0 by addition of hydrochloric acid, and ion exchange was allowed to proceed at room temperature until the pH value reached approximately 6.4. At this point, the aqueous solution of dodecylamine was added. The swollen AMH-3 was obtained after twelve hours at 60°C. As will be described in detail elsewhere, several alternative procedures failed to yield swollen AMH-3. A brief account of these attempts is shown in Figure 1.

The emergence of a swollen material was monitored by various characterization techniques. ICP (inductively coupled plasma) chemical analysis shows that Na and Sr cations of the original structure (4.8 wt% Na, 20.3 wt% Sr) were exchanged, leaving almost no Na (0.7 wt%) and a smaller

[*] S. Choi, Prof. M. Tsapatsis
Department of Chemical Engineering and Materials Science
University of Minnesota
412 Washington Ave. SE, Minneapolis, MN, 55455 (USA)
Fax: (+1) 612-626-7246
E-mail: tsapatsi@cems.umn.edu

Prof. J. Coronas
Chemical and Environmental Engineering Department
University of Zaragoza
Zaragoza 50018 (Spain)

E. Jordan, Prof. D. F. Shantz
Artie McFerrin Department of Chemical Engineering
Texas A&M University
TAMU 3122, College Station, Texas 77843 (USA)

Prof. W. Oh
Department of Nano Technology
Dong-Eui University
995 Eomgwangno, Busan 641-714 (Korea)

Prof. S. Nair
School of Chemical & Biomolecular Engineering
Georgia Institute of Technology
Atlanta, Georgia 30332 (USA)

F. Onorato
New Business and Technology Center
Pall Corporation
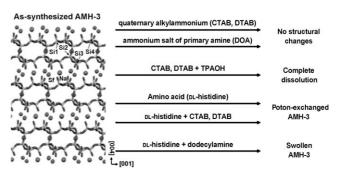Port Washington, NY 11050 (USA)

Figure 1. AMH-3 structure projection along the *b* axis showing silicon atoms (Si1, Si2, Si3, and Si4, light sticks), oxygen atoms (dark sticks), sodium cations (Na, single balls), and strontium cations (Sr, double balls). Details on the structure can be found in reference [5]. The arrows indicate attempted ion-exchange and swelling procedures. Only the last procedure, combination of ion exchange in the presence of DL-histidine and swelling using dodecylamine, resulted in swollen AMH-3. CTAB = cetyltrimethylammonium bromide, DTAB = dodecyltrimethylammonium bromide, DOA = dodecylamine, TPAOH = tetrapropylammonium hydroxide.

amount of Sr (3.1 wt%). Figure 2 includes X-ray diffraction (XRD), ^{29}Si magic-angle spinning (MAS) NMR spectroscopy, and scanning (SEM) and transmission (TEM) electron microscopy data. The FTIR spectroscopic analysis is provided
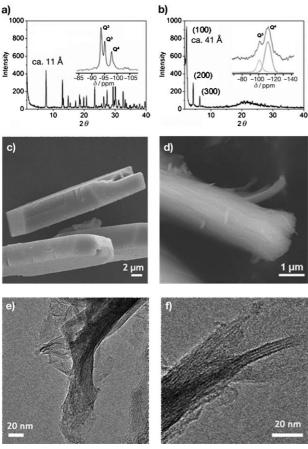

Figure 2. a, b) X-ray diffraction patterns and ^{29}Si solid-state MAS NMR spectra (inset) of original crystalline (a) and swollen (b) AMH-3. c, d) SEM images of original (c) and swollen (d) AMH-3. e, f) TEM images of swollen AMH-3.

in the Supporting Information. The unit cell of original AMH-3 includes two microporous layers and two gallery spaces, which are aligned perpendicular to the [100] crystallographic direction.[5] The first XRD peak at $2\theta \approx 7.75°$ is the (200) reflection of the AMH-3 structure (Figure 2a). The corresponding basal spacing of approximately 11.4 Å is the sum of a layer thickness and a gallery height. The layered characteristics of swollen AMH-3 are revealed by a series of new peaks at $2\theta \approx 2.14°$, 4.29°, and 6.43° indexed as (100), (200), and (300), respectively (Figure 2b). From these peaks, the basal spacing of swollen AMH-3 is calculated to be approximately 41.3 Å. Occupancy by dodecylamine molecules results in a significant increase of the gallery height, possibly facilitated by the hydrogen-bonding interaction between the layer surface silanol groups and the functional group of the primary amine. The basal spacing of swollen AMH-3 is quite close to that of swollen montmorillonite, a material with comparable layer thickness to AMH-3, intercalated by the same surfac-

tant.[25] Considering the diameter (ca. 3.2 Å) and the length (ca. 14.9 Å) of a dodecylamine molecule, it appears that the long-chain surfactant adapts a bilayer configuration within the gallery space.[25,26] Results from thermogravimetric analysis (TGA) reveal that the amount of interlayer dodecylamine corresponds to approximately 24 wt% of the swollen material.

Structural changes that occurred during the swelling process were also investigated with spectroscopic studies. ^{29}Si MAS NMR spectroscopy has been known to provide structural information on the zeolite frameworks in terms of the connectivity of SiO$_4$ tetrahedra as well as the Si-O-Si bond angles.[12,27–32] Three resonances in the original AMH-3 at $\delta = -89.4$, -90.8, and -93.5 ppm were previously assigned to the Q^3 (Si3 + Si4), Q^3 (Si1), and Q^4 (Si2) species, respectively, resulting in a Q^3/Q^4 ratio of 3:1 (Figure 2a, inset).[5,6] These chemical shifts are several ppm lower than those of typical silicates, thus implying smaller Si-O-Si angles in the AMH-3 structure.[27–29] On the other hand, NMR spectra of the swollen material (Figure 2b, inset) are quite different from those of original AMH-3, while they are comparable to those found in protonated layered silicates, such as H$^+$-magadiite.[33] Swollen AMH-3 displayed two strong resonances at $\delta = -105$ (Q^3) and -115 ppm (Q^4), with a Q^3/Q^4 ratio of 1:2.6. Changes in the chemical shifts suggest that the Si-O-Si bond angles change upon swelling, while the Q^3/Q^4 ratio changes indicate that new Q^4 species were produced by the condensation of Q^3 species. In the structure of the original AMH-3, each silicate layer is built of two oxide sheets (i.e. sublayers) wherein the Si2 centers in adjacent sublayers are bridged to form Q^4 sites.[5,6] Negative charges of the siloxy (SiO$^-$) groups on the layer surfaces, corresponding to the Q^3 species (Si1, Si3, and Si4), are coordinated to Sr and Na cations located in the gallery space (Figure 1).[5,6] In the original AMH-3, the presence of these cations imposes structural restraints, such as unusual bond angles. Substitution of gallery cations upon swelling leads to changes of the strained framework in a way that may be similar to that proposed for the protonated magadiite, that is, inversion and condensation of SiO$_4$ tetrahedra.[33] Two possible scenarios for layer structure upon swelling are proposed in the Supporting Information and discussed below.

Figure 2c displays an SEM image of crystalline AMH-3 and shows well-defined morphology of plate-like crystals. In swollen AMH-3, the overall particle shape is retained (Figure 2d). However, the well-defined compact shape of the crystalline material is lost. Instead of a flat surface, the swollen material reveals serrated edges which look like a stack of thin plates. Considering the unit cell dimension of AMH-3, the thickness of a single planar substructure is comparable to that of a few silicate layers. Each lamella runs parallel to the *bc* plane of the original crystal, that is, the same plane that contains the original AMH-3 nanoporous layer. Details in the stratified substructure can be further examined by TEM imaging (Figure 2e,f). The dark contrast in the image corresponds to the layer of silicate, while the bright region is attributed to the organic surfactant molecules occupying interlayer space. Each substructure shown in SEM imaging is composed of few silicate layers separated by amine molecules.

Communications

The ordered arrangement of silicate layers explains the appearance of new characteristic XRD peaks.

The SEM and TEM data presented above show that AMH-3 swelling occurs without disintegration of the silicate layers. However, despite the mild conditions used for ion exchange and swelling, the local order and connectivity of AMH-3 layers is not preserved, since the Q^3/Q^4 ratio changes drastically. It is unclear if this process involves only intralayer condensation of Q^3 sites (i.e. sites that in the original crystalline AMH-3 belong to the same silicate layer), thus preserving the 8 MR pores, or if more drastic rearrangements that alter the layer porosity are involved. In either case, however, structural changes during this process indicate that swollen AMH-3 should be regarded as a new material rather than an intercalated phase. Although further characterization is needed to identify the structure of the layer, possible structures (described in the Supporting Information) involving Q^3-site intralayer condensation are consistent with the available data, including N_2 adsorption data to be reported elsewhere.[34] Despite this uncertainty, we proceeded to incorporate the swollen derivative of AMH-3 into polymer nanocomposites to investigate its potential as a selectivity-enhancing additive.

A low-permeability material, polybenzimidazole (PBI), was chosen as a continuous phase, owing to its promise for use in membranes for fuel cells and gas separation. To enhance the dispersion of swollen AMH-3, a priming technique was used. The microstructure of prepared nanocomposites was characterized by TEM and XRD. Cross-sectional TEM imaging of the nanocomposite films reveals the presence of platelike particles (Figure 3a). Particles with approximately 100-nm circular contrasts were characterized by tilting to evaluate whether they are from platelike or globular particles (Figure 3b). The morphology of the dark-contrast areas changed as the tilting angle was increased, thus indicating platelike particles. This finding also suggests that the platelike particles in the nanocomposites are randomly oriented within the continuous phase of PBI. Along with the platelets of
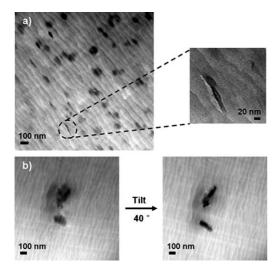

Figure 3. a) TEM images of a cross section from 3 wt% swollen AMH-3 nanocomposite. b) TEM images from tilting experiments confirming platelike morphology of silicate particles.

approximately 100-nm diameter, TEM images also reveal that a second population of smaller, globular or irregularly shaped reticular particles is present, possibly arising from the fragmentation of silicate layers. The characteristic X-ray diffraction peaks (not shown) of swollen AMH-3 disappeared by mixing with PBI. Preliminary interpretation of small-angle X-ray scattering (SAXS) data (not shown) suggests that the platelike particles are not completely exfoliated but are swollen clusters of a few AMH-3 layers.

The performance of swollen AMH-3 nanocomposite membranes was evaluated in terms of the hydrogen/carbon dioxide ideal selectivity. Figure 4 summarizes the single-gas permeation results of 2 wt% and 3 wt% swollen AMH-3
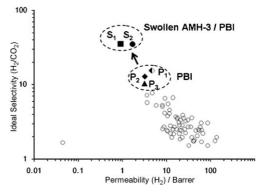

Figure 4. Hydrogen/carbon dioxide ideal selectivity versus hydrogen permeability. Pure PBI from reference [40] (P_1), pure PBI from this work (P_2), PBI with dodecylamine (P_3), and 3 wt% (S_1) and 2 wt% (S_2) swollen AMH-3/PBI nanocomposites. The open symbols denote other glassy polymers from reference [35].

nanocomposite membranes measured at 35 °C in comparison with those of pure polybenzimidazole membranes and various glassy polymers.[35] Similar to the conventional polymer-layered silicate composites, the swollen AMH-3 nanocomposite membranes exhibit permeability reduction.[36,37] However, the decrease of carbon dioxide permeability is more pronounced than that of hydrogen. As a result, at room temperature the swollen AMH-3 nanocomposite membranes show higher H_2/CO_2 ideal selectivity by a factor of two. The improvement of ideal selectivity cannot be attributed to the organic surfactant, because a PBI membrane with the same amount of dodecylamine shows similar ideal selectivity to pure polybenzimidazole membranes. The improvement is possibly due to the molecular-sieve action of the silicate additives or to the modification of the polymer properties at the polymer–silicate interfaces. If the former is the dominant factor, and considering the morphology of nanoparticles in swollen AMH-3 nanocomposites, there is room for further selectivity improvements if single exfoliated flat layers of swollen AMH-3 can be incorporated as a selective phase. The good dispersion of silicate particles also suggests that these nanoparticles could be applied in the skin layers of hollow fiber membranes fabricated with PBI.[38,39] Unfortunately, as the operating temperature of the nanocomposite membranes was increased, the permeability and selectivity improvements were reduced, so that at temperatures above 100 °C, the

© 2008 Wiley-VCH Verlag GmbH & Co. KGaA, Weinheim

behavior of the nanocomposite membranes became very similar to that of the polymer. This result may be attributed to the permeability mismatch between PBI and the silicate layer at these temperatures. Further work is directed towards exploring alternative polymers and swelling procedures.

In summary, the swollen derivative of AMH-3 was prepared, for the first time, by a novel procedure involving sequential intercalation of dodecylamine after ion exchange in the presence of amino acid. Emergence of the swollen structure is indicated by a series of new peaks in the X-ray diffraction pattern, implying bilayer configuration of the amine. SEM and TEM images indicate that particle and layer integrity are preserved during exchange and intercalation. However, the ^{29}Si MAS NMR and IR spectra suggest that structural changes occurred during the swelling process, resulting in a new silicate material. An increase in the Q^4/Q^3 ratio implies the condensation of SiO_4 tetrahedra, possibly between Q^3 tetrahedra located at opposite faces of the silicate layer. Incorporation of swollen AMH-3 into a polymer matrix leads to the disappearance of characteristic peaks in the X-ray diffraction pattern. TEM indicates that the composite contains platelike layers of nanoscale thickness along with globular or irregularly shaped reticular particles, resulting in the formation of a mixed-matrix nanocomposite. The room-temperature hydrogen/carbon dioxide ideal selectivity of swollen AMH-3/PBI nanocomposite membranes is double that of the pure polymer, possibly owing to the molecular-sieve properties of these new silicate layers.

[1] A. Corma, C. Corell, J. Perezpariente, *Zeolites* **1995**, *15*, 2.
[2] A. Corma, C. Corell, J. Perezpariente, J. M. Guil, R. GuilLopez, S. Nicolopoulos, J. G. Calbet, M. ValletRegi, *Zeolites* **1996**, *16*, 7.
[3] A. Corma, U. Diaz, V. Fornes, J. M. Guil, J. Martinez-Triguero, E. J. Creyghton, *J. Catal.* **2000**, *191*, 218.
[4] A. Corma, V. Fornes, S. B. Pergher, T. L. M. Maesen, J. G. Buglass, *Nature* **1998**, *396*, 353.
[5] H. K. Jeong, S. Nair, T. Vogt, L. C. Dickinson, M. Tsapatsis, *Nat. Mater.* **2003**, *2*, 53.
[6] S. Nair, Z. Chowdhuri, I. Peral, D. A. Neumann, L. C. Dickinson, G. Tompsett, H. K. Jeong, M. Tsapatsis, *Phys. Rev. B* **2005**, *71*, 104301.
[7] P. B. Messersmith, E. P. Giannelis, *Chem. Mater.* **1994**, *6*, 1719.
[8] P. B. Messersmith, E. P. Giannelis, *J. Polym. Sci. Part A* **1995**, *33*, 1047.
[9] A. Usuki, Y. Kojima, M. Kawasumi, A. Okada, Y. Fukushuma, T. Kurauchi, O. Kamigaito, *J. Mater. Res.* **1993**, *8*, 1179.
[10] Z. Wang, T. Lan, T. J. Pinnavaia, *Chem. Mater.* **1996**, *8*, 2200.
[11] Z. Wang, T. J. Pinnavaia, *Chem. Mater.* **1998**, *10*, 1820.
[12] J. M. Rojo, E. Ruiz-Hitzky, J. Sanz, J. M. Serratosa, *Rev. Chim. Miner.* **1983**, *20*, 807.
[13] A. Corma, V. Fornes, J. Martinez-Triguero, S. B. Pergher, *J. Catal.* **1999**, *186*, 57.
[14] M. Tsapatsis, S. Nair, H. K. Jeong, U. S. Patent, 6,863,983 (B2), **2006**.
[15] M. Tsapatsis, S. Nair, H. K. Jeong, U. S. Patent, 7,087,288 (B2), **2006**.
[16] S. Konduri, S. Nair, *J. Phys. Chem. C* **2007**, *111*, 2017.
[17] A. Corma, U. Diaz, M. E. Domine, V. Fornes, *J. Am. Chem. Soc.* **2000**, *122*, 2804.
[18] A. Corma, V. Fornes, U. Diaz, *Chem. Commun.* **2001**, 2642.
[19] Z. Wang, T. J. Pinnavaia, *J. Mater. Chem.* **2003**, *13*, 2127.
[20] O. Kwon, K. Park, S. Jeong, *Bull. Korean Chem. Soc.* **2001**, *22*, 678.
[21] P. Reichert, H. Nitz, S. Klinke, R. Brandsch, R. Thomann, R. Mulhaupt, *Macromol. Mater. Eng.* **2000**, *275*.
[22] Y. J. He, G. S. Nivarthy, F. Eder, K. Seshan, J. A. Lercher, *Microporous Mesoporous Mater.* **1998**, *25*, 207.
[23] K. Ohtsuka, *Chem. Mater.* **1997**, *9*, 2039.
[24] J. S. Dailey, T. J. Pinnavaia, *Chem. Mater.* **1992**, *4*, 855.
[25] O. Kwon, K. Park, *J. Ind. Eng. Chem.* **2001**, *7*, 44.
[26] Z. Y. Chen, X. P. Guo, Q. Zhang, J. E. Qu, *J. Mater. Sci.* **2006**, *41*, 5033.
[27] L. Rees, *Nature* **1983**, *303*, 204.
[28] J. V. Smith, C. S. Blackwell, *Nature* **1983**, *303*, 223.
[29] S. Ramdas, J. Klinowski, *Nature* **1984**, *308*, 521.
[30] R. H. Jarman, *J. Chem. Soc. Chem. Commun.* **1983**, 512.
[31] J. M. Rojo, E. Ruiz-Hitzky, J. Sanz, *Inorg. Chem.* **1988**, *27*, 2785.
[32] S. C. Christiansen, D. Zhao, M. T. Janicke, C. C. Landry, G. D. Stucky, B. F. Chmelka, *J. Am. Chem. Soc.* **2001**, *123*, 4519.
[33] T. J. Pinnavaia, I. D. Johnson, *J. Solid State Chem.* **1986**, *63*, 118.
[34] S. Choi, J. Coronas, J. A. Sheffel, E. Jordan, W. Oh, S. Nair, D. F. Shantz, M. Tsapatsis, *Microporous Mesoporous Mater.* **2007**, in press.
[35] J. Y. Park, D. R. Paul, *J. Membr. Sci.* **1997**, *125*, 23.
[36] H. K. Jeong, W. Krych, H. Ramanan, S. Nair, E. Marand, M. Tsapatsis, *Chem. Mater.* **2004**, *16*, 3838.
[37] K. Yano, A. Usuki, A. Okada, *J. Polym. Sci. Part A* **1997**, *35*, 2289.
[38] K. Y. Wang, T. Chung, R. Rajagopalan, *Ind. Eng. Chem. Res.* **2007**, *46*, 1572.
[39] K. Y. Wang, T. Chung, *J. Membr. Sci.* **2006**, *281*, 307.
[40] B. S. Jorgensen, J. S. Young, B. F. Espinoza, U.S. Patent, 6,946,015 (A1), **2004**.